RL-TR-91-433
Interim Report
December 1991

APPLICATION OF VOLUMETRIC MULTIPLE-SCATTERING APPROXIMATIONS TO FOLIAGE MEDIA

ARCON Corporation

Douglas Tamasanis

APPROVED FOR PUBLIC RELEASE; DISTRIBUTION UNLIMITED.

Rome Laboratory
Air Force Systems Command
Griffiss Air Force Base, NY 13441-5700

This report has been reviewed by the Rome Laboratory Public Affairs Office (PA) and is releasable to the National Technical Information Service (NTIS). At NTIS it will be releasable to the general public, including foreign nations.

RL-TR-91-433 has been reviewed and is approved for publication.

APPROVED:

ZACHARY O. WHITE
Project Engineer

FOR THE COMMANDER:

JOHN K. SCHINDLER
Director
Electromagnetics & Reliability Directorate

If your address has changed or if you wish to be removed from the Rome Laboratory mailing list, or if the addressee is no longer employed by your organization, please notify Rome Laboratory (ERAA) Hanscom AFB MA 01731-5000. This will assist us in maintaining a current mailing list.

Do not return copies of this report unless contractual obligations or notices on a specific document require that it be returned.

REPORT DOCUMENTATION PAGE

Form Approved
OMB No. 0704-0188

1. AGENCY USE ONLY (Leave Blank)	2. REPORT DATE	3. REPORT TYPE AND DATES COVERED
	December 1991	Interim -----

4. TITLE AND SUBTITLE
APPLICATION OF VOLUMETRIC MULTIPLE-SCATTERING APPROXIMATIONS TO FOLIAGE MEDIA

5. FUNDING NUMBERS
C - F19628-89-C-0186
PE - 62702F
PR - 4600
TA - 14
WU - 2G

6. AUTHOR(S)
Douglas Tamasanis

7. PERFORMING ORGANIZATION NAME(S) AND ADDRESS(ES)
ARCON Corporation
260 Bear Hill Road
Waltham MA 02154

8. PERFORMING ORGANIZATION REPORT NUMBER
N/A

9. SPONSORING/MONITORING AGENCY NAME(S) AND ADDRESS(ES)
Rome Laboratory (ERAA)
Hanscom AFB MA 01731-5000

10. SPONSORING/MONITORING AGENCY REPORT NUMBER
RL-TR-91-433

11. SUPPLEMENTARY NOTES
Rome Laboratory Project Engineer: Zachary O. White/ERAA/(617) 377-3191

12a. DISTRIBUTION/AVAILABILITY STATEMENT
Approved for public release; distribution unlimited.

12b. DISTRIBUTION CODE

13. ABSTRACT (Maximum 200 words)

Representation of natural terrain growth as a complex dielectric slab with some arbitrary thickness equivalent to the mean height of the vegetation is a common modeling simplification technique. The vegetation medium may be viewed as two or more different types of dielectric scatterers arranged in a random geometric configuration in a surrounding "host" medium. Based on this assumption, the foliage is treated as a continuous medium, with the propagation of the waves governed by an effective dielectric constant, (ϵ^*). In this paper several volumetric multiple-scattering models were used to determine the effective dielectric constants representative of foliage media. A brief discussion of the Average T-Matrix Approximation (ATA) and the Coherent Potential Approximation (CPA) is presented. The ATA represents the field at an individual scattering center in terms of an equivalent field produced by the other scatterers but includes no provision for the interaction between scatterers. The CPA neglects the difference between the

14. SUBJECT TERMS
Effective dielectric constant, Multiple scattering, Attenuation
Dielectric slab model, Propagation, Foliage, Electromagnetic

15. NUMBER OF PAGES
48

16. PRICE CODE

17. SECURITY CLASSIFICATION OF REPORT	18. SECURITY CLASSIFICATION OF THIS PAGE	19. SECURITY CLASSIFICATION OF ABSTRACT	20. LIMITATION OF ABSTRACT
UNCLASSIFIED	UNCLASSIFIED	UNCLASSIFIED	UL

Block 13 (ABSTRACT) (Cont'd)

external excitation field and the average field and includes interaction effects between scatterers. The effective parameters obtained using these approximations are contrasted with results obtained using several other mixing formulas. In this paper the multiple scattering approximation techniques are used to quantitatively estimate ϵ^* for vegetation media based on the foliage density and dielectric properties of the scattering elements comprising the foliage. Additionally, a formalism is presented that allows incorporation of the propagation losses experienced by an electromagnetic wave propagating through vegetation media into electromagnetic scattering models, and yet is not computationally intensive. The theoretical approximations of ϵ^* are compared with data at four levels. First, the calculated values of ϵ^* were compared with values reported in the literature. Second, skin depth penetration distances were calculated and compared to experimental values. Thirdly, the effective dielectric constants for a foliage environment were used to calculate attenuation coefficients of coherent waves propagating through dense vegetation. The calculated attenuation constants were compared with experimental measurements reported by various authors at frequencies between 50MHz and 3.2GHz, resulting in good agreement. Finally, the values of ϵ^* were incorporated into a bistatic scattering model which was used to calculate an effective normalized scattering cross section σ° for a grass and forest covered terrain. This was compared with L-band data resulting in excellent agreement between theory and experimental data.

Contents

Illustrations

Tables

1.0 INTRODUCTION

The problem of determining the attenuation loss experienced by an electromagnetic (EM) wave propagating through a foliage environment is important and quite complex. One common method used to model this phenomenon is the continuous medium approach where the attenuation properties in a foliage medium are governed by an effective dielectric constant (ϵ^*). A simple model, applying dielectric mixing formula, has been developed which can quantitatively estimate the effective dielectric constants of a foliage layer based on several descriptive parameters of the foliage media. The theoretical approximations of ϵ^* obtained from the model are compared with data at four levels. First, direct comparison of calculated effective parameters with values for similar conditions reported in the literature. Second, values of skin depth penetration calculated using the effective parameters were compared with experimentally measured values. Third, estimations of the attenuation loss (dB/m) of coherent waves propagating through a dense forest were compared with experimental data reported by various authors at frequencies between 50MHz and 3.2GHz. Finally, values of ϵ^* were incorporated into a bistatic scattering model which was used to calculate an effective normalized scattering cross section (σ°) for a sod field, grass and forest covered terrain. This was compared with L-band data resulting in excellent agreement between theory and experimental data.

The model assumes that a vegetation medium may be viewed as two or more different types of dielectric scatterers arranged in a random geometric configuration in a surrounding "host" medium. The use of an effective dielectric constant ϵ^* permits a heterogeneous mixture of random scattering elements to be treated as a homogeneous medium and provides a simple mechanism to account for multiple scattering events expected to occur when an electromagnetic wave propagates through that medium. This paper applies several multiple scattering approximation techniques to estimate values representative of ϵ^* of a vegetation medium based on readily measured quantities such as the foliage density and dielectric properties of the scattering elements comprising the foliage, i.e. wood, leaves; and presents a formalism that allows the reader to incorporate the propagation loss of an electromagnetic wave into complex electromagnetic scattering models, and yet is not computationally intensive.

A brief discussion of the general theory of the multiple scattering models that are applied in determining the values of ϵ^* is presented in Appendix A. Principal formula discussed include the Average T-Matrix Approximation (ATA) and Coherent Potential Approximation (CPA). The ATA represents the field at an individual scattering center in terms of an equivalent field produced by the other scatterers but includes no provision for the interaction between scatterers. The CPA neglects the difference between the external excitation field and the average field and includes interaction effects between scatterers. In addition, several other mixing formula are presented in order to compare the effects that differing modeling assumptions and variation of the assumed shapes of the embedded scatterers have on the determination of the effective dielectric constants.

Additionally, Appendix B includes a discussion of the methods used to obtain the dielectric constants of the components that comprise vegetation media (i.e. leaves and wood). These values are known[1,2] to be variant with respect to the moisture content and salinity of the wood, ambient air temperature, type of wood, and orientation of the wood grain with respect to the electric field polarization. Although variation of any of these conditions would cause alteration of the calculated effective dielectric constants, detailed analysis of these effects are not included in this paper which is intended to demonstrate the viability of using the multiple-scattering models to determine estimates of the effective dielectric constants of vegetation media, not on determining the values of ϵ^* for various vegetation environments.

2.0 PROPAGATION OF EM WAVES THROUGH FOLIAGE

A limited number of studies have been done that examine the multiple scattering and absorption events expected to occur when electromagnetic waves propagate in a foliage medium. Some treat each component of the vegetation as an individual scatterer and define a shape and dielectric constant associated with it[1,3,4] while others treat the foliage as a heterogeneous ensemble of scatterers of arbitrary shape and orientation[5,6,7,8]. In many instances, however, application of these processes in a system simulation program is impractical due to their complexity or computational requirements. Because of this, various assumptions are usually introduced. One common simplification involves the representation of natural terrain growth as a complex dielectric slab with some arbitrary thickness equivalent to the mean height of the vegetation. In this model the vegetation

components are considered individual scatterers embedded in a host medium. Based on this assumption, the foliage is treated as a continuous medium, with the propagation of the waves governed by an effective dielectric constant, ϵ^*. When considering propagation through and scattering from vegetation alone, use can be made of the experimental fact that the volume fraction occupied by the foliage is usually less than 5%, i.e. the foliage is sparse[9]. Another assumption made in the modeling of the propagation through and scattering from foliage is that the scattering from the interconnects between leaves and branches and leaves and stalks can be neglected. As pointed out by Brown[1], this is a good assumption since the component elements of foliage are much better absorbers of EM energy than scatterers of EM energy in the frequency range of interest here (50MHz to 3GHz). Because the foliage is sparse and absorption rather than scattering is the primary interaction process, the coherent field is dominant over the incoherently scattered waves within the medium.

The total field inside a vegetation medium can be mathematically divided into the sum of a mean or coherent part, and a zero mean fluctuating part[10],

$$\vec{\mathbf{E}} = <\vec{\mathbf{E}}> + \delta\vec{\mathbf{E}}_{fluc} \quad , \tag{1}$$

where $<\cdot>$ denotes an ensemble average and $\delta\vec{\mathbf{E}}$ is a zero mean field quantity. In order to apply effective parameters to describe the absorption and scattering of electromagnetic waves from a vegetation environment, certain conditions must be met. First, the average field $<\vec{\mathbf{E}}>$ must be much greater than the fluctuation field $\delta\vec{\mathbf{E}}_{fluc}$ having zero mean,

$$<\vec{\mathbf{E}}> >> \delta\vec{\mathbf{E}}_{fluc} \quad . \tag{2}$$

Secondly, the difference between the wave numbers of the wave propagating in the vegetation medium and in free space should be less than the reciprocal of the maximum dimension of the embedded scatterers[11],

$$(k - k_0) \cdot L < 1.0 \quad . \tag{3}$$

For spherical embedded scatterers L will be the on the order of the diameter of the spheres. The limitations of the frequency and scatterer dimension on the

determination of the effective parameters of foliage media in this study will be bounded by,

$$(\sqrt{\epsilon^*} - 1)\left(\frac{2\pi}{\lambda}\right)\cdot L \leq 0.5 \quad , \tag{4}$$

where ϵ^* is the effective complex dielectric constant of the foliage medium, L is the largest dimension of the embedded scatterers, and λ is the wavelength of the incident radiation. The condition given by Eq. (4) essentially requires that the scattering properties of a body in free space and in the random medium not be substantially different, a reasonable assumption for foliage media, which has effective dielectric constants close to that of free space[12].

If the above conditions are met, ϵ^* can be used to estimate the amplitude of an electric field that has propagated some distance through a heterogeneous random medium. The amplitude of the resulting electric field is defined by the relationship,

$$\vec{E} = \vec{E_0} \cdot \exp\left(jk_0\sqrt{\epsilon^*}\cdot z\right) \quad , \tag{5}$$

where $k_0=2\pi/\lambda$, $\vec{E_0}$ is the amplitude of the incident electric field, $\vec{E}$ is the amplitude of the electric field after propagating through the media, ϵ^* is the effective complex dielectric constant of the media, and z is the distance the wave travels through the media. The slab model is most useful when applied in a system simulation program where the foliage media represents an attenuation factor and is not the primary focus of the model. For example, when modeling the scattering from a vegetation covered terrain the vegetation layer would be represented by the homogeneous dielectric slab that covers the ground, which itself could be represented by a rough surface model. An example of an application similar to this is discussed in the section entitled "Application of the Dielectric Slab Model" later in this report. The dielectric slab model has been shown to provide a good estimate of the scattering and absorption of electromagnetic radiation propagating through foliage media when used in such a "background configuration" up to L-Band[13,14].

3.0 THEORY

Various analytical techniques have been developed in an attempt to

determine effective parameter values to describe heterogeneous media composed of a host medium and various embedded scatterers[3,5,15,16]. Few of these methods have been applied to the determination of the effective parameters of foliage media. One method that appears to be well suited to this application is the recent work of Blankenship[5], Lang[17] and Kohler and Papanicolaou[18], that extend the earlier work of M. Lax[19] and is used as the basis for this analysis.

Assume we are given a region, or scattering medium, $\mathcal{O}$ comprised of free-space with relative dielectric constant (ϵ_0=1) that contains m different embedded scatterers with relative complex dielectric constants $\epsilon_1,\ldots,\epsilon_m$. Defining V_{ij}, i = 1,...m, j = 1,2,...N_j, as the subset of $\mathcal{O}$ occupied by embedded scatterers j of class i, the dielectric properties of the composite medium occupying $\mathcal{O}$ are defined by Blankenship[2],

$$\epsilon(x) = \epsilon_0 + \sum_{i=1}^{m}(\epsilon_i-\epsilon_0)\sum_{j=1}^{N_i}\chi_{v_{ij}}(x) \quad , \tag{6}$$

where,

$$\chi_{v_{ij}}(x)=\begin{cases} 1 \text{ for } & x \in V_{ij} \\ 0 \text{ for } & x \notin V_{ij} \end{cases} \quad . \tag{7}$$

Assume that δ_i is defined to be a dimensionless parameter describing a particular aspect of the elementary scatterers in class i, such as the radius of spherical scatterers; and ρ_i is the total volume fraction of $\mathcal{O}$ occupied by scatterers of class i = 1,...,m. Given a field incident on the region $\mathcal{O}$, the objective is to characterize the scattering properties of the composite medium for the limit $N_i \rightarrow \infty$, $\delta_i \rightarrow 0$, and where ρ_i is a constant. Using the transition operator convention to derive various approximations it is possible to solve for ϵ^* of a foliage medium which can be defined as a host medium containing multiple embedded scattering types. Two such approximations are examined in this paper. The Average T-matrix Approximation (ATA) which represents the field at an individual scattering center in terms of an equivalent field produced by the other scatterers but includes no provision for the interaction between scatterers and the Coherent Potential Approximation (CPA) which neglects the difference between the external excitation field and the average field and includes interaction effects between scatterers. The effective parameters obtained using the ATA and CPA approximations are contrasted with results obtained using several other mixing

models. A detailed discussion of the approximation methods applied herein is presented in Appendix A.

4.0 DIELECTRIC CONSTANTS OF FOREST COMPONENTS

The relative dielectric constant effectively relates the polarization and conduction effects to field quantities inside and outside an object. It is usually a complex quantity and can be expressed as,

$$\epsilon = \epsilon' + j\epsilon'' \quad , \tag{8}$$

where ϵ' is the relative permittivity and ϵ'' is the loss factor resulting from propagation in a lossy medium. The loss factor accounts for losses arising from polarization phenomena in the medium (an exp(-jωt) time dependence of the fields is assumed).

Application of the approximation methods used in this study to determine the effective parameters of a vegetation environment requires a priori knowledge of the dielectric properties of the individual scatterers embedded within the host medium, as well as those of the host medium itself (air in this study). Experimental measurement of ϵ of the materials that make up a natural terrain or forest are scarce[20,21], although several models describing these values exist in the literature[2,22,23]. The values of ϵ are known to vary with respect to the moisture content, type of material (i.e. wood, leaves, etc.), ambient air temperature, wood grain orientation to the electric field polarization, as well as several other parameters. Calculation of the effective parameters presented here are representative of a nominal hard wood vegetation media. The relative dielectric constants of the forest components were estimated using models that calculate these values as a function of the physical characteristics of the components (i.e. moisture content, salinity, etc.) and the environmental conditions. It was the lack of reliable experimental data reporting measured values of the dielectric constants of the components of vegetation media that prompted the use of models to determine these values. When experimental values of the dielectric constants of foliage components for similar conditions to those used in this report were available, they were used for a comparison with the model results. The values of ϵ used in this analysis correspond to values determined for specific conditions with the intent of showing common values that can be expected in a foliage medium,

and are not professed to be universal for all forest stands. The intention was to estimate values of ϵ^* for specific vegetation environments using nominal values for the vegetation components. This would require the reader to vary these values in order to apply the formalism to a particular situation of interest. Detailed discussion of the models used to determine ϵ for the various vegetation components, and the quantitative results of these calculations, are presented in Appendix B.

5.0 CALCULATION OF EFFECTIVE DIELECTRIC CONSTANTS

The suitability of the approximation methods to estimate the effective dielectric constants of specific foliage media is first examined by comparing values of ϵ^* calculated using the models with similar values reported in the literature[12,24]. A computer program that calculates the values of ϵ^* by applying the mixing models discussed in Appendix A was developed on a DEC VAX9000 computer system. The program, in its present form, produces plots of Re(ϵ^*) and Im(ϵ^*) versus the volume fraction of an embedded scatterer. If there are multiple embedded scatterers comprising the heterogeneous medium, the model is capable of varying the volume fraction of only one of the embedded scatterers in any one calculation. Because in most cases wood will represent up to 95% of the total embedded scatterer volume fraction in a vegetation environment, the wood volume fraction was the scatterer varied in all of the example calculations presented.

Model estimates of the effective permittivity and loss factor for a forest environment composed of hardwood tree types with the wood grain perpendicular to the electric field polarization and ambient temperature of 23°C are shown in Figures 1 and 2, respectively. The plots depict the approximated values of ϵ^* of a forest environment for an incident radiation frequency of 1.3GHz. The dielectric constants of the wood and leaves comprising the vegetation were obtained using the values discussed in Appendix B. The volume fraction of the leaves in Figures 1 and 2 was assumed to be 0.001, and the volume fraction of the wood was varied from 0.0001 to 0.1. The plot contains five curves showing the results of calculations using four different shaped scatterers; spherical (ATA and CPA), needles (Polder), cylinders (Rayleigh), and disks (Bruggeman). It is apparent that the estimations provided by the ATA and CPA show good agreement with one another while agreement between the models defined for different shapes of embedded scatterers

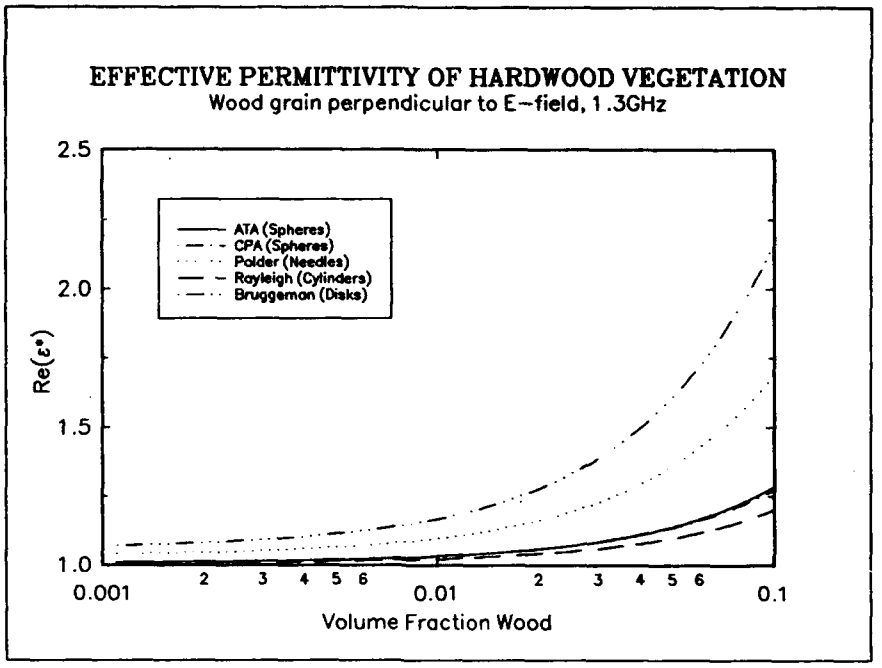

Figure 1. Effective permittivity $Re(\epsilon^*)$ of living hard wood vegetation media with the wood grain oriented perpendicular to the electric field polarization @ 23°C.

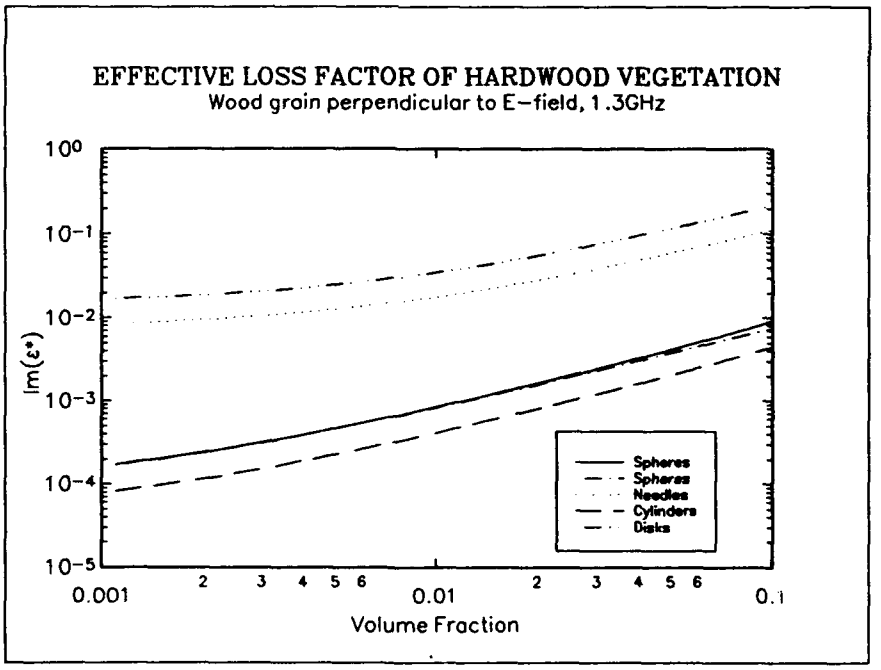

Figure 2. Effective loss factor $Im(\epsilon^*)$ of living hard wood vegetation media with the wood grain oriented perpendicular to the electric field polarization @ 23°C.

differ widely as would be expected. The cylinder shaped scatterers produce the lowest values of ϵ^* while the disk scatterers produce the highest. The magnitude of ϵ^* using needle shaped scatterers is in between the approximations for spherical and disk shaped scatterers.

Model estimates of the effective permittivity and loss factor for a forest environment composed of hardwood tree types with the wood grain parallel to the electric field polarization at a temperature of 23°C are shown in Figures 3 and 4, respectively. The plots depict the approximated values of ϵ^* for the same environmental conditions as presumed in figures 1 and 2. Observation of the parallel wood grain curves reveal that ϵ^* retains the same relative magnitudes for differing scatterer shapes as that of the perpendicular wood grain curves with the disk model returning the highest estimate and the cylinder scatterer model the lowest.

Comparison of the perpendicular and parallel wood grain curves reveals that the values of $\mathrm{Re}(\epsilon^*)$ for the parallel wood grain are consistently greater than those of the perpendicular wood grain. The increase is only slight for the sphere and cylinder curves and is much greater for the disk and needle curves. For the plots of $\mathrm{Im}(\epsilon^*)$, the spherical and cylinder perpendicular curves are consistently greater than the corresponding parallel curves versus volume fraction, while the difference between the disk and needle perpendicular $\mathrm{Im}(\epsilon^*)$ curves and the corresponding parallel curves appears to increase with increasing volume fraction, with the parallel $\mathrm{Im}(\epsilon^*)$ values being greater. The variation in the relative magnitudes of ϵ^* based on electric field orientation are expected for the different embedded scatterer shapes. A disk or needle would most certainly scatter differing amounts of energy based on its orientation relative to the electric field polarization, while spherical scatterers would scatter the same amount of energy regardless of orientation.

Effective dielectric constant versus volume fraction curves (not shown) similar to those in figures 1 through 4 were generated for a variety of incident radiation frequencies and several different values of the dielectric constant of the embedded scatterers (representing different wood types, moisture content of wood, salinity, etc.). All of these curves demonstrated the same relationship between the magnitudes of ϵ^* relative to the shapes of the embedded scatterers and wood grain orientation to the electric field polarization. The changes in the values of ϵ^* relative to alteration of the dielectric constants of the embedded scatterers resulted

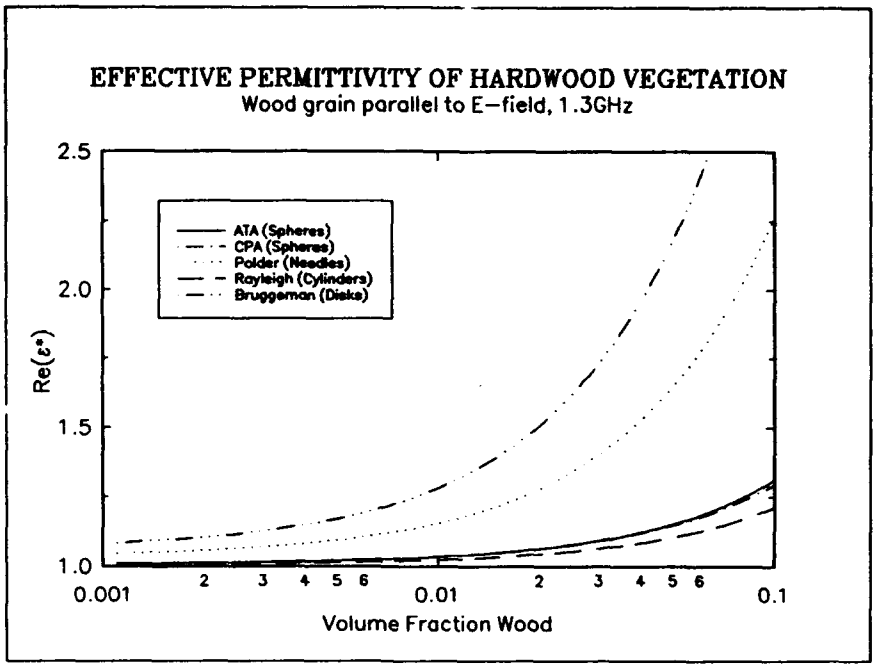

Figure 3. Effective permittivity Re(ε) of living hard wood vegetation media with the wood grain parallel to the electric field polarization @ 23°C.*

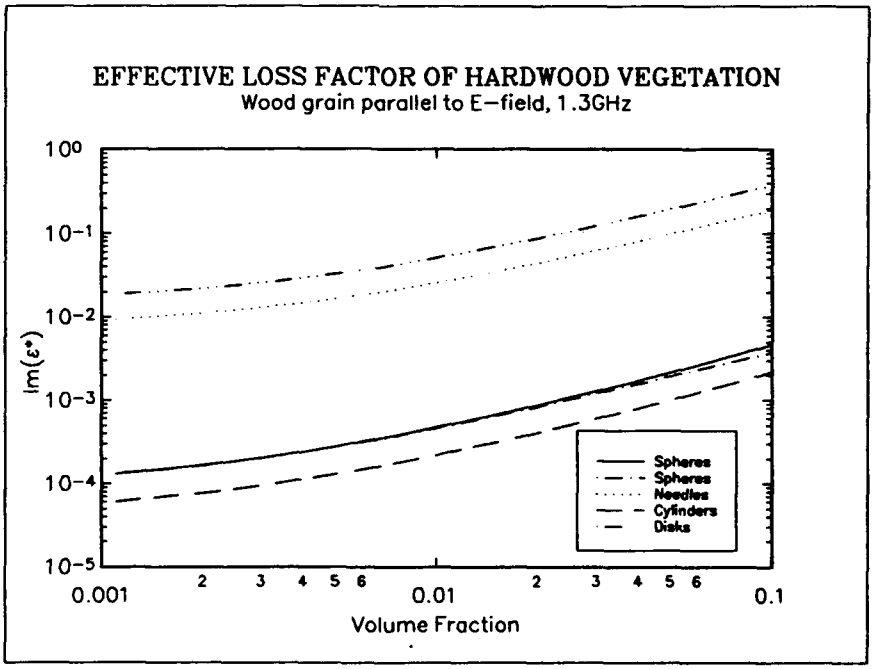

Figure 4. Effective loss factor Im(ε) of living hard wood vegetation media with the wood grain parallel to the electric field polarization @ 23°C.*

in only subtle changes in values of $\mathrm{Re}(\epsilon^*)$ and somewhat more pronounced changes in $\mathrm{Im}(\epsilon^*)$. The dominant variable affecting the values of ϵ^* is the volume fraction of the embedded scatterers.

6.0 COMPARISON OF MODEL PREDICTION WITH ESTABLISHED VALUES

The magnitude of the effective parameters of foliage media reported in the literature[12,20,25] (where the effective parameters were on the order of $1.1 + j10^{-4}$) correspond best with the values of ϵ^* calculated using the spherical embedded scatterers (i.e. the ATA and CPA). The values obtained by the disk and needle shaped embedded scatterer models were much larger than those generally reported and ranged from $1.07 \leq \mathrm{Re}(\epsilon^*) \leq 2.2$ to $1.9(10^{-2}) \leq \mathrm{Im}(\epsilon^*) \leq 2.0(10^{-1})$ and $1.04 \leq \mathrm{Re}(\epsilon^*) \leq 1.7$ to $8.5(10^{-3}) \leq \mathrm{Im}(\epsilon^*) \leq 1.0(10^{-1})$ for volume fractions of $.001 \leq \rho \leq .05$, respectively. The values obtained by the cylinder shaped embedded scatterer models were smaller than those reported in the literature and ranged from $1.006 \leq \mathrm{Re}(\epsilon^*) \leq 1.1$ and $8.1(10^{-5}) \leq \mathrm{Im}(\epsilon^*) \leq 1.0(10^{-3})$ for volume fractions of $.001 \leq \rho \leq .05$. The major discrepancy appears in the complex term of ϵ^* which can vary by an order of magnitude or more over the range of volume fractions examined.

volume fraction	embedded scatterer shape			
	sphere	needle	cylinder	disk
0.001	1,426	29	2,973	15
0.01	293	14	569	7
0.02	158	9	308	5
0.05	68	5	124	3

Table 1. Skin depth penetration in feet of a 1.3GHz wave propagating in vegetation.

To provide a tangible measure of the effect that the variations in the magnitude of ϵ^* has on the approximation of the propagation loss, estimates of the skin depth penetration were calculated using the different approximations of ϵ^*. Eq.(5) was used to determine the skin depth penetration of a 1.3GHz wave in foliage media using the values of ϵ^* reported in figures 1 and 2. Table 1 presents the results of these calculations for various density foliage environments from very sparse (0.1%) to very dense (5.0%). All values shown in table 1 reflect propagation through foliage when the wood grain is perpendicular to the electric field polarization (i.e. horizontal polarization). Examination of table 1 reveals that the needle and disk models produce effective parameters that greatly under-estimate

the experimentally measured values of the skin depth penetration in foliage media, which is reported to be between 50 and 100 feet in dense foliage[26,27], while the spherical and cylinder approximations provide a more realistic estimate of the penetration depth. The skin depth penetration calculated using the effective parameters returned by the CPA resulted in a penetration of 300 feet in a normal vegetation medium and 70 feet in a very dense vegetation medium, while the effective parameters based on the cylinder model produced skin depth penetration distances that were roughly twice those of the spherical model estimates. Experimental measurements of the propagation of a 1.3GHz wave in foliage media[28,29] verify that the estimates of the spherical model represent the best approximation of the true attenuation.

Agreement between the CPA and ATA techniques introduces the question of how important the multiple scattering processes are in a vegetation medium. Since the ATA includes no provision for the interaction between scatterers while the CPA does, if the multiple scattering interaction were a dominant process within the medium there should be a noticeable difference between these approximation methods. Since there is little or no difference, it can be concluded, based on the results of the model calculations, that multiple scattering interactions within the vegetation medium at certain frequencies are nearly negligible.

It may also be concluded from observation of figures 1 and 2 that the value of ϵ^* is extremely dependent on the volume fraction of the embedded scatterers which is representative of the density of the foliage. In some cases the magnitude of $\mathrm{Im}(\epsilon^*)$ can increase two orders of magnitude for a sparse versus dense forest environment. The magnitude of $\mathrm{Re}(\epsilon^*)$ is also dependent on the volume fraction of the embedded scatterers but to a much lesser degree (also see Table 1).

6.1 Comparison of Model Prediction with Experimental Data

As another measure of the validity of the effective parameters calculated, a comparison with experimentally measured values of the attenuation coefficient (α in dB/m) reported in the literature was done. Experimental measurement of the attenuation coefficients of EM waves propagating in vegetation media reported in the literature are rare. Four sources were found that contained measurements of the attenuation coefficients that were used for comparison to the data from this analysis.

First, a comparison of the calculated attenuation coefficients (α in dB/m) based on the effective parameters of the four embedded scatterer shape models was done. The results of this calculation were plotted versus the frequency of the incident radiation and are shown in figure 5. These values represent horizontally

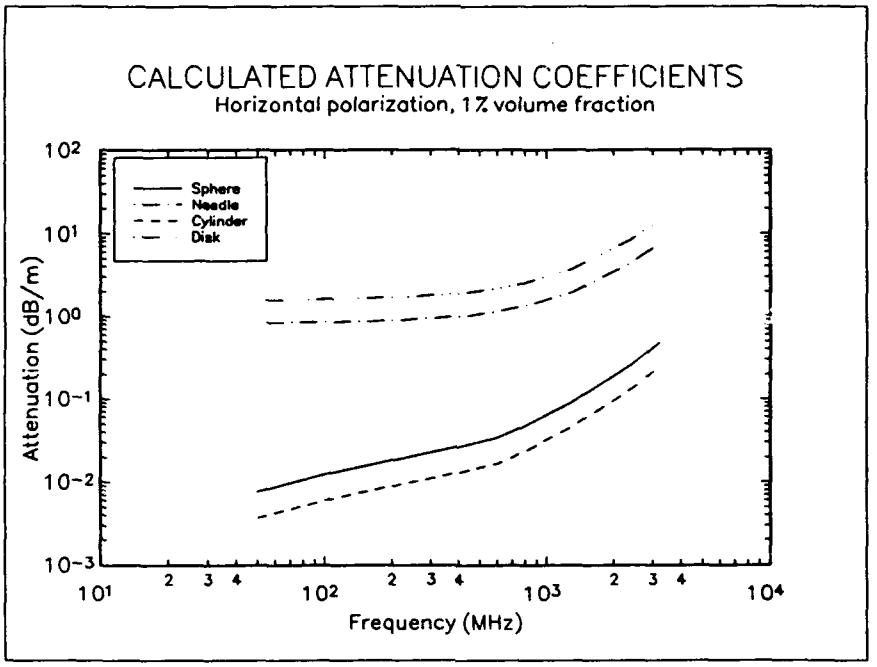

Figure 5. Relationship between α (dB/m) calculated for various assumed embedded scatterer shapes for a 1.3GHz wave in a normal density foliage environment.

polarized waves propagating through a normal density foliage medium at an ambient air temperature of 23°C. As with the skin depth calculation, the models based on the disk and needle embedded scatterers produced attenuation coefficients much greater than those obtained by the spherical and cylinder based models. Determination of which of these models provides the best estimate of the propagation loss is verified by comparison of the calculated attenuation coefficients with experimentally measured values. From this comparison it was concluded that the effective parameters calculated using the CPA provided the best estimate of α. Figures 6 and 7 present a comparison of the measured and calculated attenuation coefficients for horizontal and vertical polarized waves, respectively.

Figure 6 depicts the attenuation coefficients calculated using the CPA for embedded scatterer volume fractions of 1% and 5% compared to experimental measurements of these values from four sources[28,29,30]. The measured values

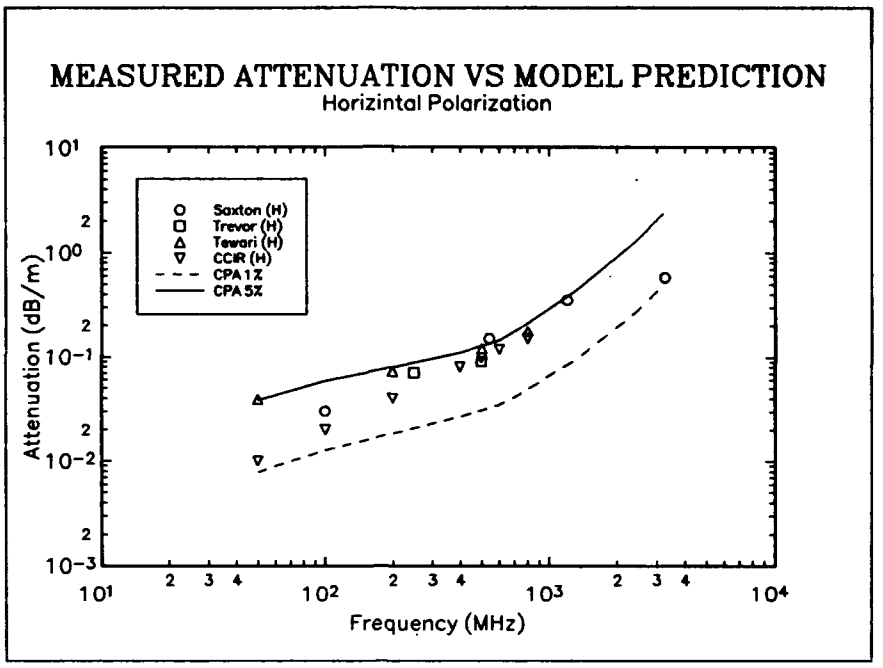

Figure 6. Comparison of model estimates of α (dB/m) with experimentally measured values for dense foliage. Horizontal polarization.

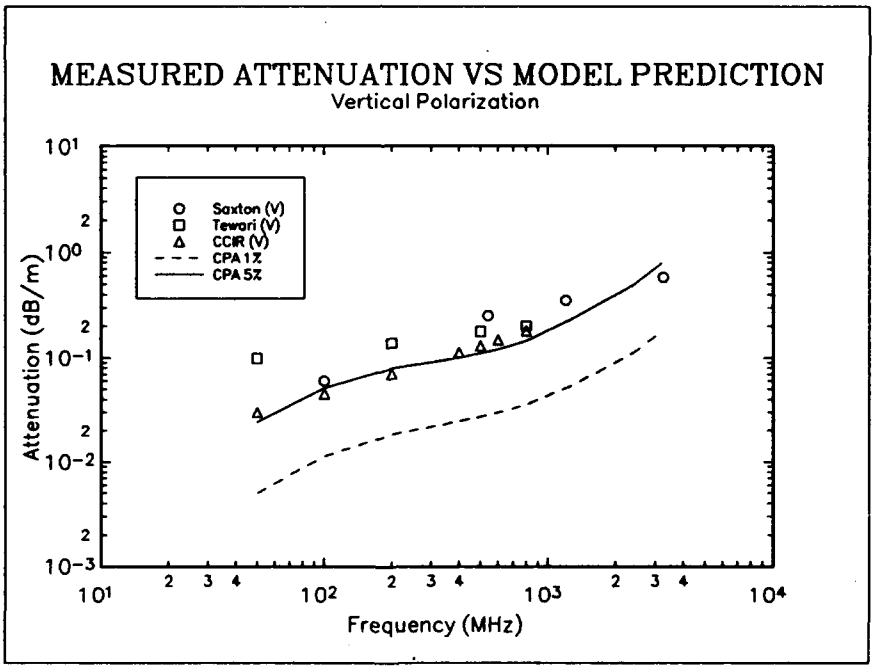

Figure 7. Comparison of model estimates of α (dB/m) with experimentally measured values for dense foliage. Vertical polarization.

represent the attenuation loss of horizontally polarized waves propagating in dense foliage. The calculated values appear to provide a good estimate of the attenuation as the majority of the experimentally measured points fall between the 1% and 5% curves. As would be expected the experimental values are near the upper curve because all of the measured values represent propagation through what was described as very dense foliage. It is apparent from the figure that the best agreement between the model estimates and experimental measurements occurs between the frequency limits of 50MHZ to 1GHz. In this range the experimentally measured values appear to fall within the 1% to 3% volume fraction range expected of dense foliage. At lower frequencies the model appears to agree with some measurements while underestimating others. At frequencies above 1GHz, the model appears to provide reasonable estimates of the attenuation even though the frequency limitations of the mixing models begin to become apparent somewhere in the 1GHz to 3GHz range. There is a large disparity between experimentally measured values of the attenuation coefficients at certain frequencies. In some cases this disparity is greater than the difference between the model prediction and measured data. The difference between the experimentally measured and model predicted values could be attributed to any one of several possible factors that could contribute to natural variation in the dielectric properties of the vegetation media in which the measurements were taken. Essentially, variation in the dielectric properties of the components comprising different vegetation environments, and even within vegetation environments, prevent consistently accurate determination of the attenuation properties of vegetation media by experimental or theoretical means.

Figure 7 shows the attenuation coefficients calculated using the CPA for embedded scatterer volume fractions of 1% and 5% compared to experimental measurements of these values by three sources. The measured values represent the attenuation loss of vertically polarized waves propagating in very dense foliage. The values calculated based on the model do not provide as good an estimate of the attenuation of the vertically polarized waves as for the horizontally polarized waves. Although several of the experimental points fall on or near the 5% curve, the majority of the experimentally measured points are above the 5% curves. True volume fraction values would not be expected to be much above 1% to 3% in practical terms, which means that the model will underestimate the attenuation loss for vertically polarized waves. The greater underestimation of the attenuation

coefficients of the vertically polarized waves than the horizontally polarized waves can be attributed to the greater depolarization effects that vertical waves experience compared to horizontal waves when propagating through vegetation[30]. This reveals an inherent weakness in the effective medium approximation technique which does not account for polarization related scattering effects resulting from differently shaped embedded scatterers in the foliage and relies solely on the variation of the dielectric constants of the embedded scatterers to account for polarization effects.

The general shapes of the curves in figures 6 and 7 appear to mimic the trends exhibited by the reported experimental data versus frequency. The magnitude errors could be attributed to poor estimates of the dielectric constants of the embedded scatterers comprising the foliage medium compared to the true values of the forests where the propagation measurement were taken. Dielectric constants of the foliage components can be expected to vary from forest to forest as well as spatially within a forest. Therefore, better estimates of the composition of a vegetation media will lead to better approximations of the dielectric constants of the components which will result in better estimates of the effective parameters.

Overall, the effective dielectric constants calculated using the CPA will provide a good estimate for of the attenuation loss of a horizontally polarized wave and a fair estimate of a vertically polarized wave propagating in a vegetation media. The frequency bounds are difficult to verify based on the results shown in figures 6 and 7. Given the accuracy of the CPA model estimates of the effective parameters, use of the other approximation techniques would clearly result in either much to great an attenuation loss, in the case of the needle and disk models, or much to little attenuation, in the case of the cylinder based model.

6.2 Application of the Dielectric Slab Model

As a final test of the suitability of the effective parameters, calculated using the CPA, to model attenuation through vegetation, the results of the application of the slab model[31] in a scattering simulation are shown. In this simulation, a transmitting antenna and receiving antenna are located over a surface with two scales of roughness that is covered by a foliage layer. Both the coherent and incoherent power scattered into the receiver are calculated. The model assumes only in-plane scattering; there is no out-of-plane aziumthally dependent scattering.

Waves are launched from the transmitting antenna down to the foliage covered terrain. Each ray from the transmitting antenna is treated as a plane wave whose amplitude is weighted by the pattern factor of the transmitting antenna. Each wave in the angular spectrum of plane waves emanating from the transmitter is ray traced through the foliage layer down to the rough surface, is reflected, and then ray traced back up through the foliage layer and into a bistatic receiving antenna. The rough surface scattering is governed by the two scales of roughness model of Peake-Barrick[31]. Only the mean value of the electric field (coherent part) is ray traced down through the foliage layer. The coherent wave reflected from the rough surface is ray traced back up through the foliage layer and is amplitude weighted by the pattern factor of the receiving antenna. Also, the diffuse EM energy reflected from the rough surface is composed of an angular spectrum of waves, each of which is ray traced up through the foliage layer, suffers some attenuation, and is then amplitude weighted by the pattern factor of the receiving antenna. In this investigation, the theoretical model, with appropriate rough surface parameters, was used to predict an effective normalized cross section σ° which is then compared with experimental data. The comparisons shown here are for three terrain types: a grass covered field, a forest and a flooded forest. The agreement between the theoretical model and the data is, in general, quite good.

Figures 8 and 9 show L-Band scattering data (σ° vs. θ_i) for a 1-meter grass field taken with a SAR[32]. The theoretical model calculations were performed with the following surface parameters: σ_L=1.22 m, T_L=5 m, σ_s=3.16$\cdot 10^{-2}$ m, T_s=4.0$\cdot 10^{-2}$m, where ϵ(ground) = 30.0+j0.6 and ϵ^*(grass)=1.2+j0.005. Figure 8 shows the excellent agreement between the SAR data and the theoretical model for HH polarization for the grass covered field. Figure 9 shows moderately good agreement between theory and data for the VV polarization for the grass covered field. The 5 dB discrepancy may be due to some depolarization for the VV polarization (the vertically polarized incident EM waves are partly scattered into horizontally polarized waves).

Figure 10 shows two data points (σ°) for a sparse forest ($\simeq$ 22 m trees) from a SAR with HH polarization. One data point (the solid circle) corresponds to a normal forest[32], and falls very near the theoretical model curve. The surface parameters used in the theoretical model curve are given as follows: σ_L=1.22m, T_L=10.0m, σ_s=3.16$\cdot 10^{-2}$m, and T_s=4.0$\cdot 10^{-2}$m, while ϵ(ground)= 30.0+j0.6 and ϵ^*(forest) = 1.03+j0.0002. The second data point (the empty circle) in Fig. 10

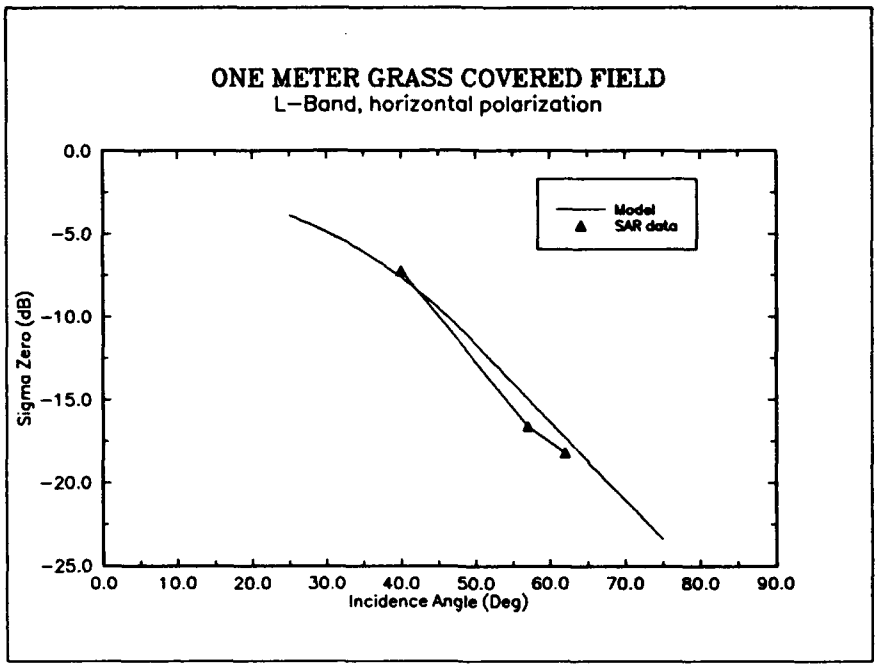

Figure 8. Comparison of model predicted σ° values with measured SAR data for a 1 meter grass field at L-Band and horizontal polarization.

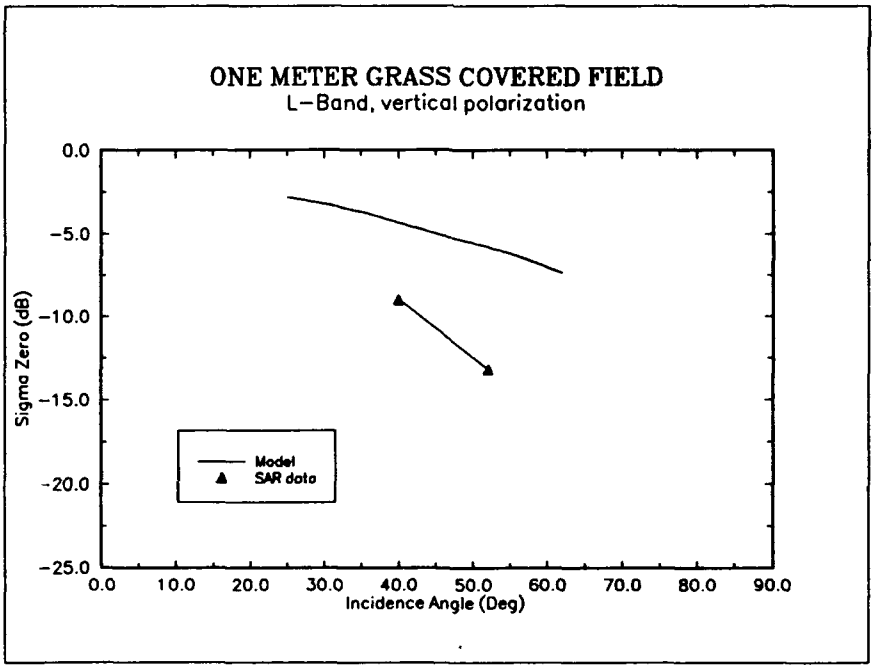

Figure 9. Comparison of model predicted σ° values with measured SAR data for a 1 meter grass field at L-Band and vertical polarization.

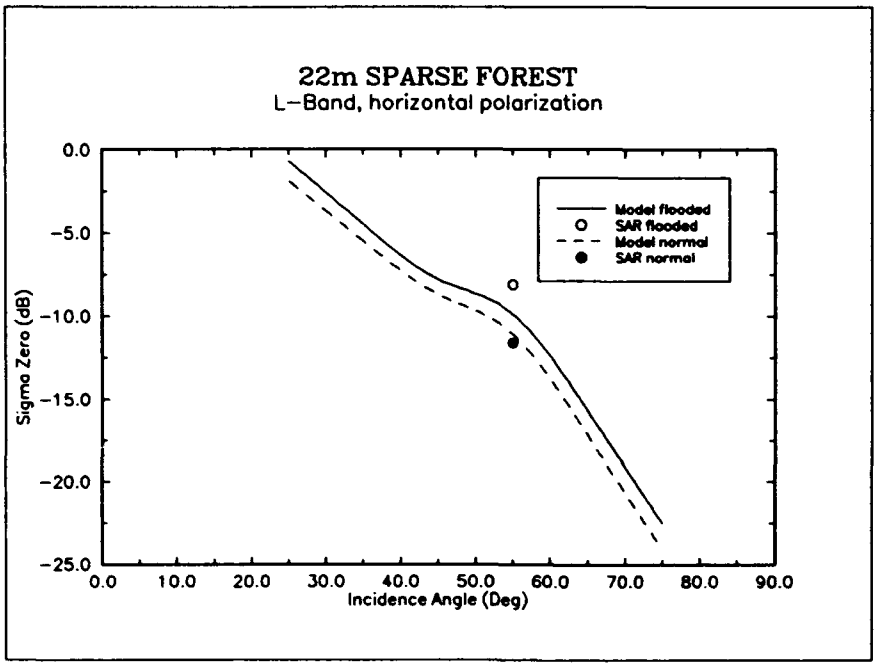

Figure 10. Comparison of model predicted σ° values with measured SAR data for a 22 meter forest at L-Band and horizontal polarization.

corresponds to σ° for the same forest ($\simeq$ 22 m trees) flooded. The theoretical model surface parameters are the same as for the normal forest, but with ϵ(ground)= 80.0+j0.6 (corresponding to lake water). The agreement of the data[16] with the theoretical model is quite good (within 3dB). The theoretical model also shows the same trend as the data points, the σ° for the flooded forest is several dB higher than σ° for a normal forest.

In Fig. 11, several L-Band data points for σ° from a forest comprised of 10m trees are shown versus incidence angle θ_i for HH polarization[33]. The surface parameters used in the theoretical calculations are as follows: σ_L=1.22m, T_L=10.0m, σ_s=$3.16 \cdot 10^{-2}$m, T_s=$4.0 \cdot 10^{-2}$m, where ϵ(ground)=30.0+j0.6 and ϵ(forest)=1.03+j0.0002. The agreement of the data with the theoretical model is again quite good. The most statistically significant point of the measured data corresponds to the value of σ° at an incidence angle of 55°. This is also where the theoretical model curve nearly intersects the data curve.

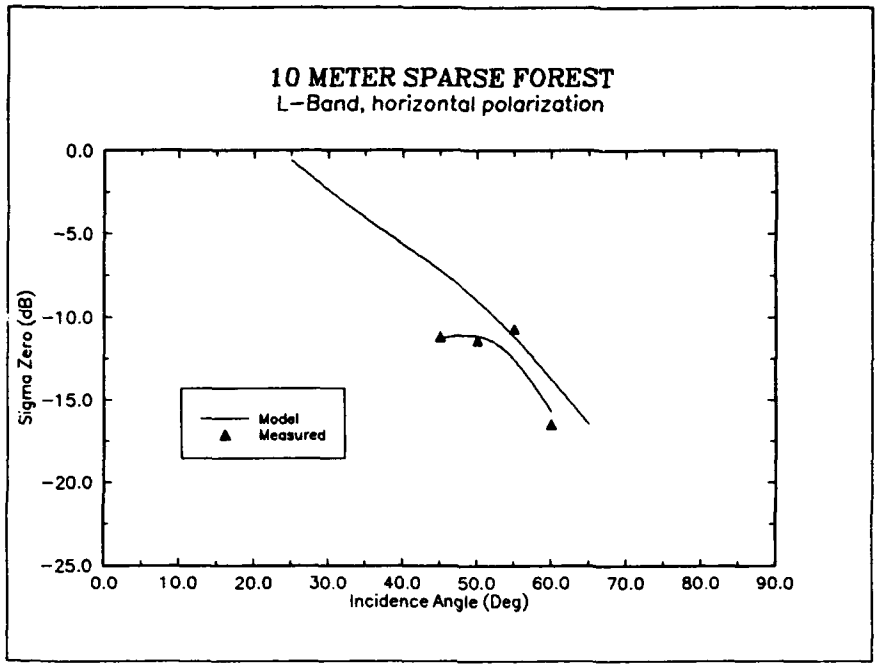

Figure 11. Comparison of model predicted σ° values with measured data for a 10 meter forest at L-Band and horizontal polarization.

7.0 CONCLUSION

Based on the overall agreement between the model approximations and experimental data, the effective dielectric constants calculated using the Average T-Matrix Approximation and the Coherent Potential Approximation provide the basis for a reasonable formalism to predict the propagation loss of an electromagnetic wave propagating through a vegetation environment. Values of the effective dielectric constants calculated agree well with the values currently accepted in the literature. In addition, the calculated attenuation coefficients of waves propagating through vegetation media and experimental measurements of these values agree quite well. Finally, as demonstrated by the bistatic scattering model output (figures 8-11), the dielectric slab model will provide a good estimate of the amplitude loss of a coherent electromagnetic wave propagating through foliage. The formalism is not computationally intensive and yet accounts for the effects of multiple scattering phenomenon and is, therefore, appealing for use in large scale system simulation programs where computation time has to be minimized. Use of this formalism as the primary method to determine the propagation effects of a wave propagating great distances through foliage media is

not recommended. The model is primarily intended to provide a secondary attenuation factor attributable to the presents of vegetation. That is, to be applied in a system simulation program similar to the bistatic scattering model discussed in this report.

The primary variable influencing the magnitude of the effective parameters is the volume fraction of the embedded scatterers which is proportional to the density of the foliage. This effect appears to be consistent with the experimental measurements reported in the literature which do vary based on the type and condition of the vegetation but are mainly dependent on the density of the foliage.

Because of inherent limitations in the mixing model, the size of the embedded scatterers as compared to the incident radiation frequency will influence the accuracy of the model estimates of propagation loss. Therefore, application of the effective parameters will be best suited to model propagation through a forest canopy or vegetation having small diameter trunks, each of which present smaller dimension scatterers than, say, the trunks of a mature forest. Another important effect of the wavelength to embedded scatterer size is the frequency limitations of the model. It appears from the data that the model will provide good estimate of the attenuation loss up to frequencies of 3.2GHz in certain vegetation environments.

As shown in figures 6 and 7, the ability to account for specific polarization is weak. This can be primarily attributed to the lack of variation in the scattering properties of the embedded scatterers, which are assumed to be constant geometric shapes. The variation in polarization that is demonstrated is entirely attributable to the differing dielectric constants of the embedded scatterers based on the orientation of the wood grain to the electric field polarization. In addition to the inability to accurately distinguish the attenuation for differently polarized waves, the proposed formalism is only capable of determining the amplitude loss of the wave and includes no provisions to determine the phase of the wave. If necessary, the model could be expanded to include the effects of different scattering shapes and could possibly provide a better approximation of the attenuation of waves having different polarizations. At present, the approximation of the attenuation loss is sufficient for the applications for which this formalism was developed and the possible improvements gained by the expansion of the model is not considered a necessity.

REFERENCES

1. Brown, G.S., and Curry, W.J., "An Analytical Study of Wave Propagation Through Foliage", Rep. RADC-TR-79-359, Rome Air Development Center, Hanscom, AFB, Mass., *Final Technical Report*, January 1980. AD A084348

2. Yavorsky, J.M., "A Review of Electrical Properties of Wood", *Technical Publication*, no. 73, New York State College of Forestry at Syracuse University, Syracuse, NY, 1951.

3. Brown, G.S., and Curry, W.J., "A Theory and Model for Wave Propagation Through Foliage", *Radio Science*, Vol. 17, pp. 1027-1036, 1982.

4. Ruck, G.T., Barrick, D.E., Stuart, W.D., and Krichbaum, C.K., *Radar Cross Section Handbook*, Vol. 2, Plenum press, (1970).

5. Blankenship, G.L., "Stochastic Modeling of EM Scattering From Foliage", Rep. RADC-TR-89 22, Rome Air Development Center, Hanscom, AFB, MA, March 1989. AD A213118

6. Fung, A.K., and Ulaby, F.T., "A Scattering Model for Leafy Vegetation", IEEE *Trans. Antennas and Propagation*, Vol. AP-16, no. 4, pp 281-285, October 1978.

7. Lang, R.H., and Sidhu, J.S., "Electromagnetic Backscattering From a Layer of Vegetation: A Discrete Approach", *Trans. Antennas and Propagation*, Vol. GE-21, 1no. 1, pp. 62-71, January 1983.

8. Pounds, D.J., and LaGrone, A.H., "Considering Forest Vegetation as an Imperfect Dielectric Slab", Rep. no. 6-53, *Electr. Eng. Res. Lab.*, Univ. of Texas, Austin, TX (Available as AD#410836, Natnl. Inf. Serv., Springfield, VA), 1963.

9. Tamasanis, D., "Effective Dielectric Constants of Foliage Media", Rep. RADC-TR-90-157, Rome Air Development Center, Hanscom AFB, MA, 1990. AD A226296

10. Brown, G.S., "A Theoretical Study of the Effects of Vegetation on Terrain Scattering", Rep. RADC-TR-88-64, Rome Air Development Center, Hanscom, AFB, Mass., *Final Technical Report*, August 1987. AD A198781

11. Varadan, V.K.. Bringi. V.N., and Varadan, V.V., "Coherent Electromagnetic Wave Propagation Through Randomly Distributed Dielectric Scatterers", *Phys. Rev. D*, 19, pp. 2480-2486, 1979.

12. Tamir, T., "On Radio-Wave Propagation in Forest Environments", IEEE *Trans. Antennas and Propagation*, Vol. AP-15, no. 6, pp. 806-817, November 1967.

13. Golden, A., "A Foliage Penetration Study", Rep. RADC-TR-78-34, Rome Air Development Center, Hanscom AFB, Mass., 1978. AD A055391

14. Sachs, D.L., and Wyatt, P.J., "A Conducting-Slab Model for Electromagnetic Propagation Within a Jungle Medium", Defense Research Corp., *Tech. Memo.* 376 and *Internal Memo.*, IMR-471, 1966.

15. Tinga, W.R., Voss, W.A.G., and Blossey, D.F., "Generalized Approach to Multiphase Dielectric Mixture Theory", *Jour. Appl. Phy.*, Vol. 44, no. 9, pp. 3897-3902, September 1973.

16. VanBeek, L.K.H., "Dielectric Behavior of Heterogeneous Systems", *in Progress in Dielectrics*, Vol. 7, Ed. Birks, J.B., Chemical Rubber Company, Cleveland, OH, 1967.

17. Lang, R.H., "Electromagnetic Backscattering From a Sparse Distribution of Dielectric Scatterers", *Radio Science*, Vol. 16, no. 1, pp. 15-30, January 1981.

18. Kohler, W.E., and Papanicolaou, G.C., "Some Applications of The Coherent Potential Approximation", *in Multiple Scattering and Waves in Random Media*, Eds. Chow, P.L., Kohler, W.E., Papanicolaou, G.C., North-Holland, New York, pp. 199-223, 1981.

19. Lax, M., "Multiple Scattering of Waves", *Rev. Mod. Phys.*, Vol. 23 pp. 287-310, 1951, and *Phys. Rev.*, Vol. 85 pp. 621-629, 1952.

20. Broadhurst, M.G., "Complex Dielectric Constants and Dissipation Factor of Foliage", NBS *Report* no. 9592, NBS project 3110107, US Naval Ordnance Laboratory, October 1970, (Distribution Unlimited).

21. Skaar, C., "The Dielectric Properties of Wood at Several Radio Frequencies", *Technical Publication*, no. 69, Vol. XXI, no. 1-d, New York State College of Forestry at Syracuse University, Syracuse, NY, 1948. (Distribution Unlimited)

22. Brown, G.S., "Coherent Wave Propagation Through a Sparse Concentration of Particles," *Radio Science*, Vol. 15 No. 3, (1980).

23. James, W.L., "Dielectric Properties of Wood and Hardboard: Variation With Temperature, Frequency, Moisture Content and Grain Orientation", USDA *Forest Service Res. Paper* FPL 245, USDA Forest Products Lab., Madison, MI, 1975.

24. Ulaby, F.T., Moore, R.K., and Fung, A.K., *Microwave Remote Sensing Active and Passive*, Vol. I, II, III, Artech House, 1986.

25. McPetrie, J.S., and Ford, L.H., "Some Experiments on the Propagation of 9.2 cm Wavelength, Especially on the Effects of Obstacles, *Jour.* IEE, Vol. 93, Part III A, pp. 531, 1946.

26. Megaw, E.C.S., "Some Effects of Obstacles on the Propagation of Very Short Radio Waves", *Journal* IEE, pp.97-105, 1947.

27. Saxton, J., and Lane, J., "Dielectric Dispersion in Pure Polar Liquids at Very High Radio Frequencies, III," in The Effect of Electrolytes in Solution, *Proc. Roy. Soc.*, 214A, pp. 531-545, 1952.

28. Travor, B., "Ultra-High-Frequency Propagation Through Woods and Underbrush", RCA *Review*, Vol. 5, pp. 97-100, July 1940.

29. Tewari, R.K., Swarup, S., and Roy, M.N., "Radio Wave Propagation Through Rain Forests of India", IEEE *Trans. Antennas and Propagation*, Vol. AP-31, no. 4, pp. 433-449, April 1990..

30. Papa, R.J., and Tamasanis, D., "A Model for Bistatic Scattering of Electromagnetic Waves From Foliage Covered Terrain," NATO AGARD Conference Proceedings, *Targets and Clutter Scattering and Their Effects on Military Radar Performance*, Ottowa, CA, Paper No. 4, 1991.

31. Larson, R.W., Kasischke, E.S., and Maffett, A.L., "Calibrated L-Band Terrain Measurements and Analysis Program - Results," RADC-TR-88-49, (1988) AD A196573.

32. Ulaby, F.T., and Dobson, M.C., "Handbook of Radar Scattering Statistics for Terrain," Artech House, (1989).

33. Tsang, L., Kong, J.A., and Shin, R.T., "*Theory of Microwave Remote Sensing*," John Wiley and Sons, (1985).

34. Bensoussan, A., Lions, J.L., and Papanicolaou, G.C., *Asymptotic Analysis For Periodic Structures*, North-Holland, Amsterdam, 1978.

35. Kollmann, Côtē, *Principals of Wood Science and Technology*, Springer Verlag, 1968.

36. DeLoor, G.P., "Dielectric Properties of Heterogeneous Mixtures Containing Water", *Jour. Microwave Power.*, Vol. 3, no. 2, pp 67-73, 1968.

37. Ulaby, F.T., Razani, M., and Dobson, M.T., "Effects of Vegetation Cover on the Microwave Radiometric Sensitivity to Soil Moisture", IEEE *Trans. Geoscience and Remote Sensing*, Vol. GE-21, no. 1, pp. 51-61, January 1983.

APPENDIX A

MODELS FOR THE EFFECTIVE DIELECTRIC CONSTANTS OF FOLIAGE

In this section a review of the expressions used to calculate the effective dielectric constants ϵ^* of foliage media is presented. Because the derivation of these equations are all readily available in the literature[5,9,16,18] the derivations shown here will be kept to a minimum in the interest of space.

Subject to the constraints stated in the body of the paper, the continuous medium approach, characterized by an effective dielectric constant, may be analyzed by solving the wave equation with a fluctuating (random) dielectric constant using various approximation techniques. The transition operator T is used as a basis for the various approximations in multiple scattering formalisms. Maxwell's equations are written as,

$$\nabla \cdot (\epsilon_0 \vec{\mathbf{E}}) + \sum_{i=1}^{m} (\epsilon_i - \epsilon_0) \sum_{j=1}^{N_i} \nabla \cdot (\chi_{ij} \vec{\mathbf{E}}) = 0, \tag{1}$$

and,

$$\nabla \times \vec{\mathbf{E}} = 0 \quad , \tag{2}$$

where (2) is a quasi-static approximation. Use of the quasi-static approximation assumes that the dimensions of the scatterers are much less than the wavelength of the incident radiation thus imposing an upper frequency limitation on the results of the approximation models. The frequency limitations are governed by Eq. (4) in the main body of the report, and are dependent on the frequency of the incident radiation, effective dielectric constant of the medium and dimension of the scatterers. Equation 1 implies that there are m constituents and N_i is the number of scatterers of the i^{th} type. Here, ρ_i is the volume fraction of the i^{th} type of scatterer, x is a spatial parameter and χ_{ij} is the support of the j^{th} scatterer of type i, where,

$$\chi_{ij}(x) = \begin{cases} 1 & x \text{ in } j^{th} \text{ scatterer of type } i \\ 0 & \text{otherwise} \end{cases} \quad . \tag{3}$$

The two relationships,

$$\vec{\mathbf{D}}(x) = \epsilon(x) \vec{\mathbf{E}}(x) \quad , \tag{4}$$

and,

$$\langle \vec{D}(x) \rangle = \epsilon^* \vec{E} \quad , \tag{5}$$

define ϵ^* where $< \cdot >$ denotes ensemble average.

Expressing Eq. (1) in operator form,

$$(L_0 + M)\vec{E} = 0 \quad , \quad \nabla \times \vec{E} = 0 \quad , \tag{6}$$

where,

$$L_0 = \nabla \cdot (\epsilon_0 \cdot) \, , \tag{7}$$

$$M = M_1 + \ldots + M_m \, ,$$

with,

$$M_i = \sum_{j=1}^{N_i} V_{ij} \, , \tag{8}$$

and,

$$V_{ij} = (\epsilon_i - \epsilon_0) \cdot \nabla(\chi_{ij}(\cdot)) \quad . \tag{9}$$

The T matrix may be defined as,

$$T = (L_0 + M)^{-1} M \quad . \tag{10}$$

After considerable algebraic manipulation, and expanding the T matrix in a power series and neglecting higher order multiple interaction terms, an expression for ϵ^* may be determined in terms of expectation values of the T operator and the dielectric constant[5,17].

$$\epsilon^* \sim [<\epsilon> - \sum_{i=1}^{m} <\epsilon T_i>] \cdot [I - \sum_{i=1}^{m} <T_i>]^{-1} \tag{11}$$

In addition, if it is assumed that there is only a single class of embedded scatterers (m=1) and the scatterers are spherical in shape, the following approximation for ϵ^* may be obtained[5,9]:

$$\epsilon^*(\epsilon_0;\epsilon_1,\rho_1) \simeq \frac{\langle \epsilon \rangle + \rho_1 \epsilon_1 \left(\frac{\epsilon_0 - \epsilon_1}{2\epsilon_0 + \epsilon_1}\right)}{1 + \rho_1 \left(\frac{\epsilon_0 - \epsilon_1}{2\epsilon_0 + \epsilon_1}\right)} \, . \tag{12}$$

where ϵ_0 represents the dielectric constant of the host medium, ρ_1 and ϵ_1 the

volume fraction and dielectric constant of the embedded scatterer, respectively, and

$$\langle\epsilon\rangle \triangleq (1 - \rho_1)\epsilon_0 + \rho_1\epsilon_1 \quad . \tag{13}$$

Spherical embedded scatterers, although not representative of the actual shapes of vegetation components, were used to demonstrate the effectiveness of the dielectric mixing models at estimating the values of ϵ^*. The best physical analogy between the spherical scatterer and actual vegetation components would be clumps of leaves and branches in a vegetation canopy that can be somewhat spherical or infinitely small spheres representing scattering centers at the actual point of scattering.

For low volume fractions, the average T-matrix approximation (ATA) may be written,

$$\epsilon^*(\epsilon_0;\epsilon_1,\rho_1) \simeq \epsilon_0\left(1 + 3\rho_1\left(\frac{\epsilon_1 - \epsilon_0}{2\epsilon_0 + \epsilon_1}\right) + 3\rho_1^2\left(\frac{\epsilon_1 - \epsilon_0}{2\epsilon_0 + \epsilon_1}\right)^2\right). \tag{14}$$

This approximation is good only for small volume fractions $\rho \leq 0.02$ and neglects interparticle scattering interactions.

In the coherent potential approximation (CPA), the difference between the field exciting the medium and the average field is neglected[5,9,18,34]. A reference dielectric constant ϵ_r is introduced into Maxwell's equations, and is later chosen to simplify (optimize) the equations for ϵ^*:

$$\nabla\cdot(\epsilon_r\vec{E}) + \sum_{i=1}^{m}\sum_{j=1}^{N_i}\nabla\cdot\left((\epsilon_i - \epsilon_0)\chi_{ij}\vec{E}\right) + \sum_{i=1}^{m}\sum_{j=1}^{N_i}\left(\frac{\epsilon_0 - \epsilon_r}{mN_i}\right)\nabla\cdot\vec{E} = 0 \ , \tag{15}$$

and,

$$\nabla\times\vec{E} = 0 \quad .$$

In operator notation, this is written as,

$$(L_r + M_r)\vec{E} = 0 \quad , \tag{16}$$

where,

$$L_r = \nabla\cdot(\epsilon_r\,\cdot) \quad , \tag{17}$$

$$M_r = \sum_{i=1}^{m}\sum_{j=1}^{N_i} V_{ij}^r \quad , \tag{18}$$

and,

$$V^{\Gamma}_{ij} = \nabla\cdot\left((\epsilon_i - \epsilon_0)\cdot\chi_{ij}\right) + \left(\frac{\epsilon_0 - \epsilon_r}{mN_i}\right)\nabla\cdot \quad . \tag{19}$$

The T matrix in this approximation is defined as,

$$\epsilon^* \sim [<\epsilon> - \sum_{i=1}^{m}\sum_{j=1}^{N_i}<\epsilon T_i>]\cdot[I - \sum_{i=1}^{m}\sum_{j=1}^{N_i}<T_i>]^{-1} \tag{20}$$

where,

$$T^{\Gamma}_{ij} = (L_{\Gamma} + V^{\Gamma}_{ij})^{-1}V^{\Gamma}_{ij} \quad . \tag{21}$$

After much algebraic manipulation, an expression for ϵ^* may be determined in terms of ϵ_{Γ}, and expectation values of the dielectric constant and the T^{Γ} matrix. This expression for ϵ^* greatly simplifies if ϵ_{Γ} is chosen so that[5,9,18,34],

$$< \sum_{i=1}^{m}\sum_{j=1}^{N_i} T^{\Gamma}_{ij} > = 0 \quad . \tag{22}$$

This is the CPA and requires that,

$$\frac{\epsilon_0 - \epsilon_r}{3\epsilon_r} = \sum_{i=1}^{m}\rho_i\cdot\left(\frac{\epsilon_0 - \epsilon_i}{3\epsilon_r + \epsilon_i - \epsilon_0}\right) \quad , \tag{23}$$

where $\rho_i = \frac{4}{3}\pi\delta^3 c_i$ with c_i being the average number of scattering centers of class i per unit volume. The general expression for ϵ^* obtained by solving the operator equation (20) is,

$$\epsilon^* \simeq \epsilon_0 + \left(\sum_{i=1}^{m}\rho_i\epsilon_i - \rho\epsilon_0\right) - (1-\rho)\epsilon_0\left(\frac{\epsilon_0 - \epsilon_r}{3\epsilon_r}\right) + \left(\sum_{i=1}^{m}\rho_i\epsilon_i\cdot\frac{\epsilon_0 - \epsilon_i}{3\epsilon_r + \epsilon_i - \epsilon_0}\right) - \left(\sum_{i=1}^{m}\rho_i\epsilon_i\right)\cdot\left(\frac{\epsilon_0 - \epsilon_i}{3\epsilon_r + \epsilon_i - \epsilon_0}\right) , \tag{24}$$

where,

$$\rho = \sum_{i=1}^{m}\rho_i \quad .$$

When only one class of embedded scatterer is considered (m=1) and the scatterers are very small, Eqs. (23) and (24) combine to give the CPA for ϵ^*;

$$\epsilon^*(\epsilon_0;\epsilon_1,\rho_1) \simeq \epsilon_0\left(1 + 3\rho_1\left(\frac{\epsilon_1 - \epsilon_0}{2\epsilon_0 + \epsilon_1}\right) + \rho_1^2\left(\frac{(\epsilon_1 - \epsilon_0)^2(\epsilon_1^2 + 13\epsilon_0\epsilon_1 - 5\epsilon_0^2)}{\epsilon_0(\epsilon_1 + 2\epsilon_0)^3}\right)\right). \tag{25}$$

Given the questionable correlation between the actual physical makeup of vegetation components and spherical embedded scatterers, mixing formula derived using various embedded scatterer shapes (needles, cylinders, and disks) were also examined. Following the derivation of Polder and Van Santen VanBeek[16] the generalized expression for the effective parameter of a heterogeneous dielectric mixture is expressed,

$$\epsilon\text{-}\epsilon_0 = \frac{1}{3}\, v_1(\epsilon_1\text{-}\epsilon_0) \sum_{a,b,c} \frac{\bar{\epsilon}_0}{[\bar{\epsilon}_0 + A_i(\epsilon_1\text{-}\bar{\epsilon}_0)]} \ , \tag{26}$$

where a,b,c represent the axes of the embedded scatterer, A_i is the depolarization factor along the i^{th} axis of the embedded scatterer, and $\bar{\epsilon}_0$ is specified later and must lie within the range of $\epsilon_0 \leq \bar{\epsilon}_0 \leq \epsilon$.

For long prolate spheroids $A_i = (\frac{1}{2}\text{-}\delta,\ \frac{1}{2}\text{-}\delta,\ 2\delta)$, where $\delta \ll 1$. Inserting these values for A_i into Eq.(26) leads to,

$$\epsilon = \epsilon_0 + \frac{1}{3}\, v_1(\epsilon_1\text{-}\epsilon_0)\bar{\epsilon}_0 \left(\frac{4}{(\epsilon_1\text{-}\bar{\epsilon}_0)} + \frac{1}{\bar{\epsilon}_0 + 2\delta(\epsilon_1\text{-}\bar{\epsilon}_0)} \right) \ , \tag{27}$$

Equation (27) can be solved for various scatterer shapes. The special case of $\delta \to 0$ represents embedded scatterers of long thin needles. Solved in the limits $\bar{\epsilon}_0 = \epsilon_0$,

$$\epsilon = \epsilon_1 + v_1 \frac{(\epsilon_1\text{-}\epsilon_0)(5\epsilon_0 + \epsilon_1)}{3(\epsilon_0\text{-}\epsilon_1)} \ , \tag{28}$$

Another formula obtained by Rayleigh[16] represents embedded scatterers that are rectangular cylinders with their axes parallel and perpendicular to the field direction. The resulting formula is expressed,

$$\epsilon = \epsilon_0 \frac{\epsilon_0 + \epsilon_1\text{-}v_1(\epsilon_1\text{-}\epsilon_0)}{\epsilon_0 + \epsilon_1 + v_1(\epsilon_1\text{-}\epsilon_0)} \ , \tag{29}$$

Disks can be approximately regarded as oblate spheroids. For flat extended oblate spheroids $A_i = (\delta,\ \delta,\ 1\text{-}2\delta)$, where $\delta \ll 1$. Equation 26 can be applied again to obtain a general formula to estimate ϵ for disk shaped scatterers.

$$\epsilon = \epsilon_0 + \frac{1}{3}\, v_1(\epsilon_1\text{-}\epsilon_0)\bar{\epsilon}_0 \left(\frac{2}{\bar{\epsilon}_0 + \delta(\epsilon_1\text{-}\bar{\epsilon}_0)} + \frac{1}{\epsilon_1\text{-}2\delta(\epsilon_1\text{-}\bar{\epsilon}_0)} \right) \ , \tag{30}$$

For the case when δ=0 and $A_i = (0, 0, 1)$ Eq.(30) becomes,

$$\epsilon = \epsilon_0 + \frac{1}{3} v_1 \frac{(\epsilon_1-\epsilon_0)(\epsilon_2+2\epsilon_1)}{\epsilon_1} \quad , \tag{31}$$

for $\tilde{\epsilon}_0 = \epsilon_0$. Bruggeman was the first to obtain Eq.(31) by means of his integration scheme which resulted in the following equation for disks[16],

$$\epsilon = \epsilon_1 \frac{3\epsilon_0 + 2v_1(\epsilon_1-\epsilon_0)}{3\epsilon_1 - v_1(\epsilon_1-\epsilon_0)} \quad , \tag{32}$$

It is possible to extend the case of m=1 (one embedded scatterer in a host medium) to the case of several embedded scatterers in a host medium ($m \geq 2$) by using an iterative procedure. When a background medium ϵ_0 contains the classes of embedded scatterers, ϵ_1 and ϵ_2, the effective dielectric constant of the medium can be defined as $\epsilon^*(\epsilon_0;\epsilon_1,\rho_1/(1 - \rho_2))$ where the embedded particles are characterized by (ϵ_2,ρ_2). An alternate to this would be to determine the effective dielectric as $\epsilon^*(\epsilon_0;\epsilon_1,\rho_2/(1 - \rho_1))$ where the embedded scatterers are characterized by (ϵ_1,ρ_1). This recursive technique constructs models of media containing several classes of scatterers by embedding the "next" class of scatterers into a medium whose effective parameters have been derived for the "previous" classes of scatterers[2].

For the case of two embedded scatterers where the volume fractions, ρ_1 and ρ_2, are in the low to moderate range,

$$\epsilon^*(\epsilon_0;\epsilon_1,\rho_1;\epsilon_2,\rho_2) \simeq \epsilon^*\left(\epsilon^*\left(\epsilon_0;\epsilon_1,\frac{\rho_1}{(1 - \rho_2)}\right);\epsilon_2,\rho_2\right) \quad , \tag{33}$$

or,

$$\epsilon^*(\epsilon_0;\epsilon_1,\rho_1;\epsilon_2,\rho_2) \simeq \epsilon^*\left(\epsilon^*\left(\epsilon_0,\epsilon_2,\frac{\rho_2}{(1 - \rho_1)}\right);\epsilon_1,\rho_1\right) \quad , \tag{34}$$

will yield good approximations of ϵ^* of the composite medium. The terms $\rho_1/(1 - \rho_2)$ and $\rho_2/(1 - \rho_1)$ in Eqs. (33 and 34) represent the effective volume fractions of the intermediate mixtures of (ϵ_0,ϵ_1) and (ϵ_0,ϵ_2), respectively. When $\rho_1 < \rho_2$, Eq. (33) will be the preferred approximation and if $\rho_2 < \rho_1$, Eq. (34) will be the preferred approximation.

To compute ϵ^* of a medium with M classes of embedded scatterers, a technique similar to "iterated homogenization" is applied[35]. One can determine the approximation of $\epsilon^*(\epsilon_0;\epsilon_1,\rho_1; \ldots ;\epsilon_m,\rho_m)$, where $\rho_i \leq \rho_{i+1}$, by recursively adding

scatterers to the "new" background medium in order of increasing density. The effective volume fraction of a scatterer of type j in the medium defined by the background medium and the first j scatterers ($\epsilon_0,\epsilon_1,\ldots,\epsilon_j$) may be expressed,

$$\rho_j^{-M} \triangleq \frac{\rho_j}{1 - \sum_{j=1}^{M} \rho_j} \quad . \tag{35}$$

Using this expression, the estimate of ϵ^* can be expressed as[5],

$$\begin{aligned}
\epsilon^*(\epsilon_0;\epsilon_1,\rho_1;\ldots;\epsilon_M,\rho_M) &\simeq \epsilon^*\left(\epsilon^*\left(\epsilon_0;\epsilon_1,\frac{\rho_1}{(1-\rho_M)}\right);\ldots;\epsilon_{M-1},\frac{\rho_{M-1}}{(1-\rho_M)}\right);\epsilon_M,\rho_M\right) \\
&\simeq \epsilon^*\left(\epsilon^*\left(\epsilon^*\left(\epsilon_0;\epsilon_1,\frac{\rho_1}{(1-\rho_M-\rho_{M-1})}\right);\ldots;\epsilon_{M-2},\frac{\rho_{M-2}}{(1-\rho_M-\rho_{M-1})}\right);\epsilon_{M-1},\frac{\rho_{M-1}}{(1-\rho_M-\rho_{M-1})}\right);\epsilon_M\rho_M\right) \\
&\simeq \epsilon^*\left(\epsilon^*\left(\ldots\epsilon^*\left(\epsilon^*(\epsilon_0;\epsilon_1,\rho_1^{-M});\epsilon_2,\rho_2^{-M}\right);\ldots;\epsilon_{M-1},\rho_{M-1}^{M}\right);\epsilon_M,\rho_M\right) \quad .
\end{aligned} \tag{36}$$

APPENDIX B

DIELECTRIC PROPERTIES OF TREES

A limited number of studies have been done that experimentally or theoretically determine the dielectric properties of trees[1,2,3,20,21,23]. Despite this, reliable dielectric measurements of living wood are scarce, although some data has been compiled for dry wood or lumber. The major difference between the dielectric properties of lumber and those of living wood are attributable to the moisture content of each. Some differences could be due to sap and other nutrients within the wood that may also affect the electrolytic nature of the wood, but these effects are secondary when compared to the moisture content[22].

The model used in this analysis to determine ϵ' of wood was developed by James[11] and further enhanced by Brown[22] and includes the effects of incident polarization and frequency. Values of ϵ' of the hard and soft wood trees calculated using the model do not vary a great deal over the frequency range considered in this report. Data reported from experimental measurements of ϵ' of living wood also exhibited a leveling off above 20MHz[2,20,21]. These data do, however show a slight but constant downward trend in the magnitude of ϵ' as the frequency increases from audio to radio to infra-red frequency bands. By close examination of these data it was determined that ϵ' consistently decreased over the frequency range of interest in this study. The values of ϵ' reported in Figure 1B reflect this slight downward trend as the frequency increases. The magnitude of the changes were based on the results of experimental data reported for wood of similar densities and moisture contents[20]. The slight decrease in ϵ' as the frequency increases may be attributable to the fact that at higher frequencies the time required for polarization to occur may be equal to or even exceed the period of alternation of the applied electric field. Therefore, the magnitude of the polarization decreases resulting in a subsequent decrease in ϵ'.

The magnitude of ϵ' of living wood can be expected to increase as the ambient temperature approaches the freezing point[3]. Experimental data reported seems to substantiate the slight increase in ϵ' as temperature decreases but this conclusion was not apparent from the data in all reports cited Skaar 49, Yavorsky 51, Brown 82, and Broadhurst 70].

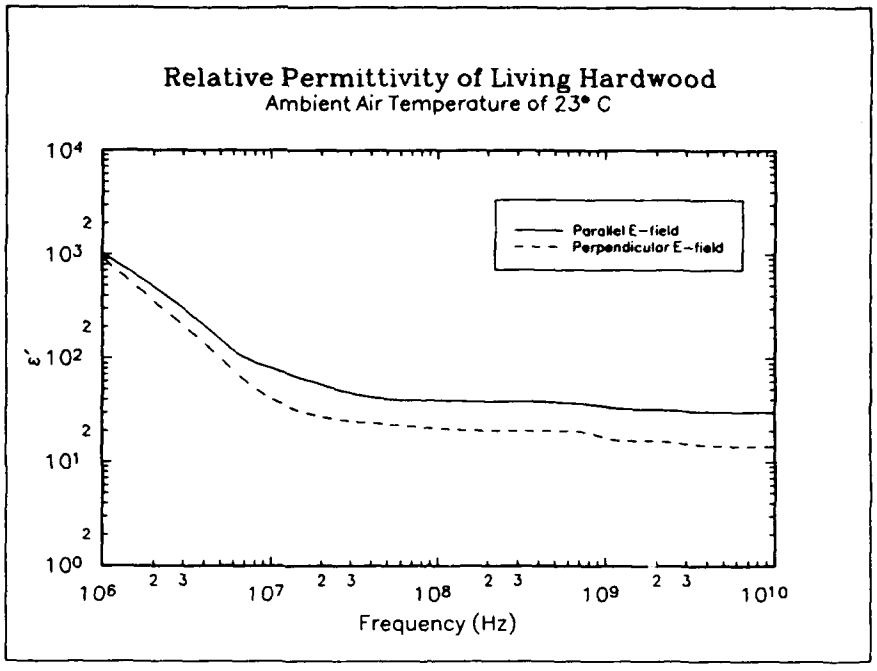

Figure 1B. Re(ϵ^*) of living hard wood with the incident radiation electric field polarization either parallel oriented or perpendicular to the wood grain orientation.

LOSS FACTOR OF WOOD

The dependence of the loss factor (ϵ'') on the physical properties of wood is more difficult to determine than that of ϵ'. A great disparity is reported to exist between the loss factor of cut wood[23] and a sample from a living tree branch[2,22]. The loss due to dipolar depolarization is sometimes the only type of loss considered in high frequency models for leaves and wood. In wood and leaves, water volume is considered to dominate the variation of ϵ'' and so a mixing type of formula is generally based on the estimates of the water volume in a unit volume of material. A model to determine the wood loss factor, accounting for each type of dominant loss phenomenon, has been derived by Brown[22] and is frequency-dependent on the incident radiation, the relaxation frequency of water and the moisture content of the wood. The results from this model compared favorably with experimental data[20], although widespread application is doubtful. The frequency dependence of ϵ'' on the radiation is quite complicated and may be considerable in magnitude. The variation of ϵ'' with respect to the temperature has been shown

experimentally[2] to decrease in moist wood as the temperature increases. This reversal is attributable to the fact that at higher temperatures the water dipoles experience less frictional effects. The correlation of ϵ'' with the wood grain orientation relative to the electric field has not been established experimentally. The loss factor as measured with an electric field parallel to the wood grain is greater than that with the electric field perpendicular to the grain as the model predicts. The reason for this behavior may be attributed to the basic structure of cellulose crystallites[2].

Values of ϵ'' of wood for conditions of interest in this study are shown in Figure 2B as a function of frequency. The calculations of these hardwood values were based on a mean moisture content of 80%, and wood density of 0.75. It is common for the wood moisture content when taken as a percentage of the oven dried weight of the wood, as defined by wood technologists and forestry professionals, to have values greater than 100%[36]. All values were determined assuming an ambient air temperature of 23°C[21,22].

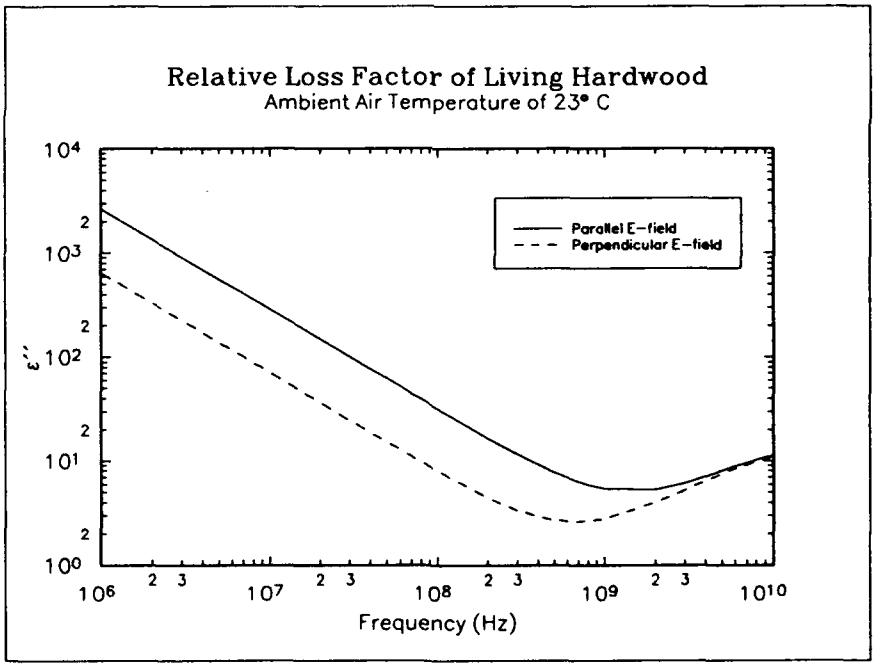

Figure 2B. Im(ϵ) of living hard wood with the incident radiation electric field polarization either parallel oriented or perpendicular to the wood grain orientation.*

COMPLEX RELATIVE DIELECTRIC CONSTANTS OF LEAVES

To obtain a valid estimate of the effective parameters of a foliage medium, values of the dielectric properties of leaves must be known. Although some reports[3] site that the leaves on leaf-bearing trees can be ignored below frequencies of 3GHz, the scope of this study includes operating frequencies near this boundary which will necessitate the inclusion of the effects of leaves. There are very few sources in the literature that provide measured data for ϵ of leaves. Those that are available[20,21] report ϵ of only certain types of leaves and for a limited number of incident radiation frequencies. To obtain approximations for these values, a modeling technique developed by DeLoor[37] that determines ϵ of leaves based on their moisture content, the ambient air temperature, and the incident radiation frequency was used. In the DeLoor model the leaf is modeled by considering the leaf to be comprised of a background medium composed of organic material, and that ellipsoidal disks of water are randomly distributed throughout this material. The model uses a dielectric mixing formula that is a function of the volume fraction of the water inclusions and ϵ of the host material and water.

The relative dielectric constants of leaves for various conditions of interest in this study have been computed and are shown in Table 1B. Assuming that the moisture content of the leaves is high for the tropical environment in which much of the experimental measurements of propagation through foliage were done, a moisture content of 65% is used in the determination of the dielectric constant of leaves in the study. The salinity of leaves can vary from 1% to 12%. As there is no way to estimate this figure for a typical forest, a value of 6% is assumed here. The moisture content and salinity used are representative of leaves at the height of the growth season. The values calculated by the model compared favorably with experimental data found in the literature[3,17,20,24,25].

	Frequency (MHz)								
	50	100	200	400	600	800	1300	2400	3200
ϵ'	44.6	44.7	44.6	44.5	44.3	44.3	44.0	43.4	43.0
ϵ''	209.0	105.0	53.0	27.0	19.0	15.0	11.0	10.0	11.0

Table 1B. ϵ' and ϵ'' of broad leaves and needles for leaves with moisture content of 65%, salinity of 6%, and ambient air temperature of 23°C.

DENSITY OF FOREST COMPONENTS

Having specified values for the electrical properties of forest constituents, quantitative values describing the density of the various foliage components must be established. A typical parameter used to define the density of foliage is the volume fraction that the foliage components occupy in a typical forest. The volume fraction is defined as the ratio of volume occupied by foliage components to the total volume of the layer containing the forest environment. Quantitative measurements of the volume fractions of forests are scarce, and determination of an estimate requires the development of sophisticated modeling programs. Although models are available to determine the volume fractions of forest stands[3,22,24], actual values of volume fractions can be expected to vary greatly depending on the region, season and weather pattern. The model in this report calculates the effective parameters as a function of the volume fraction (Figures 1 through 4) which allows determination of ϵ^* based on an estimate of the volume fraction of a forest stand of interest. Therefore, the only task is to determine a suitable range of volume fractions over which to do the calculation of ϵ^* that will be representative of a majority of forest environments.

From the literature reviewed, it was found that in the typical mature forest the wood will occupy approximately 1.0% of the total volume[2,3,22,24]. In some cases, well managed forests can attain wood volume fractions in the vicinity of 5.0%. This is considered an extreme case. For the purpose of this work, calculations will be done for wood volume fractions over a range of 0.1% to 5.0%.

The volume fraction of broad leaves or needles was typically reported to be between 10 to 25 percent of the volume fraction occupied by the wood. Therefore, the volume fractions of leaves in this report will be consistently reported as 10% of the total volume fraction, which is considered typical[3]. It is the intent to use a range of volume fractions that is significantly broad so that most forest stands, with similar vegetation composition, can be represented.

MISSION

OF

ROME LABORATORY

Rome Laboratory plans and executes an interdisciplinary program in research, development, test, and technology transition in support of Air Force Command, Control, Communications and Intelligence (C^3I) activities for all Air Force platforms. It also executes selected acquisition programs in several areas of expertise. Technical and engineering support within areas of competence is provided to ESD Program Offices (POs) and other ESD elements to perform effective acquisition of C^3I systems. In addition, Rome Laboratory's technology supports other AFSC Product Divisions, the Air Force user community, and other DOD and non-DOD agencies. Rome Laboratory maintains technical competence and research programs in areas including, but not limited to, communications, command and control, battle management, intelligence information processing, computational sciences and software producibility, wide area surveillance/sensors, signal processing, solid state sciences, photonics, electromagnetic technology, superconductivity, and electronic reliability/maintainability and testability.